Journal of Chromatography A, 1603 (2019) 412–416

Contents lists available at ScienceDirect

Journal of Chromatography A

journal homepage: www.elsevier.com/locate/chroma

Short communication

The effect of column packing procedure on column end efficiency and on bed heterogeneity – Experiments with flow-reversal

Dóra Zelenyánszki[a], Nándor Lambert[b], Fabrice Gritti[c], Attila Felinger[a,b,d,*]

[a] Department of Analytical and Environmental Chemistry and Szentágothai Research Center, Ifjúság útja 6, H-7624 Pécs, Hungary
[b] MTA–PTE Molecular Interactions in Separation Science Research Group, Ifjúság útja 6, H-7624 Pécs, Hungary
[c] Waters Corporation, Milford, MA 01757, USA
[d] Institute of Bioanalysis, Medical School, University of Pécs, Szigeti út 12, H-7624 Pécs, Hungary

ARTICLE INFO

Article history:
Received 21 March 2019
Received in revised form 20 May 2019
Accepted 22 May 2019
Available online 28 May 2019

Keywords:
Column packing
Flow-reversal
Packed bed heterogeneity
Sub-2-μm particles
UHPLC

ABSTRACT

The effect of column end structure and bed heterogeneity of six commercially available reversed-phase chromatographic columns for fast liquid chromatography with different column packing materials – such as fully porous (Waters XBridge C_{18} with 1.7 μm particles) and superficially porous (Waters CORTECS C_{18} with 1.6 μm particles), with column dimension of 2.1 × 50, 100 or 150 mm were tested with flow-reversal method. The method includes arresting the flow when a non-retained marker (thiourea) has penetrated to a given distance into the column and then reversing the column. Hence, when the flow has been restarted, the sample is eluted at the same end of the column where it entered. The experiments showed that all columns are axially heterogeneous, and some differences could be observed between the two respective column ends. Furthermore, we can conclude that the shorter columns are axially more homogeneous than the longer ones, thus the column length is an influencing factor on the column packing procedure.

1. Introduction

Ultra-high-performance liquid chromatography (UHPLC) as a method in instrumental analysis has received substantial attention during the recent years in separation science. Two specific novelties in UHPLC are the development of high-quality sub-2-μm porous particles and the availability of LC systems with pressure tolerance elevated beyond 1000 bar. With these systems, narrow-bore columns are used – with an internal diameter of no more than 2.1 mm – which are packed with sub-2-μm particles [1,2].

Besides the development of column packing materials, column packing procedures are important factors as well. The high-pressure slurry packing has been the most effective and the most widely used. By this technique, the slurry suspension of packing materials is in a reservoir, which is connected to the column. The packing solvent is passed under high pressure and high flow-rate into the reservoir to push the slurry on the column [3–5].

The procedure of slurry packing has continuously been optimized where, among other things, the viscosity, wettability, density, and dispersing ability of the packing were tested [6–9]. The flow-reversal method has been discussed in the literature sporadically. It was used for example to determine the theoretical plate heights of chromatographic columns prepared by stacked membranes and for the determination of the degree of distortion of the liquid-phase flow profile in columns for preparative liquid chromatography [10–12].

Lambert et al. studied the effects of the presence of the frits and the bed heterogeneity of packed and monolithic columns with a flow-reversal method. They found that for an unretained analyte in a well-packed column, the band broadening occurring in the homogeneous stationary phase bed and in the end structure of the column are almost identical [13].

Recently Gritti et al. [14] have designed and built a custom-made low-dispersion system made of two 50-nL optical detection cells placed immediately before and after the column to improve the accuracy of the plate height measurements. They applied the flow reversal technique to quantify radial and axial structural heterogeneities of packed chromatographic beds. Gritti and Gilar have recently studied the impact of frit dispersion in gradient elution chromatography [15]. They found that the presence of the outlet frit has a serious limitation on the achieved efficiency. Thus there are several evidences confirming that frit technology should be seriously revisited [13–15].

* Corresponding author at: Department of Analytical and Environmental Chemistry and Szentágothai Research Center, University of Pécs, Ifjúság útja 6, H-7624 Pécs, Hungary.
E-mail address: felinger@ttk.pte.hu (A. Felinger).

https://doi.org/10.1016/j.chroma.2019.05.040
0021-9673/

In our present study, the flow-reversal method has been employed to examine the bed heterogeneity at the respective column ends. Due to the nature of the column packing procedure, one may assume that the inlet and the outlet ends of the columns exhibit a different structure and efficiency [13], thus experiments were carried out to test either the column inlet or the outlet.

The columns we have tested were commercial columns packed with a slurry packing technique optimized by Waters Corporation [8]. These columns serve as the basis to understand the effect of the column length on the axial heterogeneity of packed beds and column ends.

2. Theory

The band variance is defined in various units in separation science. The second central moment μ_2 of the peaks (band variance) can be measured on time scale, which gives the temporal variance σ_t^2. The spatial variance σ_z^2 determines the longitudinal zone broadening in the column. It is calculated from the σ_t^2 the following way

$$\sigma_z^2 = \sigma_t^2 u_z^2 \quad (1)$$

where u_z is the chromatographic linear velocity of the band. The extra-column contributions are expressed in volumetric variance σ_V^2, which is calculated as

$$\sigma_V^2 = \sigma_t^2 F_v^2 \quad (2)$$

where F_v is the volumetric flow rate. It should be noted that the calculated band variances must be corrected for the effect of the extra-column band broadening σ_{system}^2. The various contributions to the overall observed band broadening are explained as

$$\sigma_{t/V}^2 = \sigma_{\text{system}}^2 + \sigma_{\text{park}}^2 + \sigma_{\text{end}}^2 + \sigma_{\text{bed}}^2 \quad (3)$$

where $\sigma_{t/V}^2$ is the total variance expressed as either temporal or volumetric variance, σ_{park}^2 is the band broadening originating from the effect of the diffusion during the peak parking period, σ_{end}^2 arises from the heterogeneity of the packed bed in the vicinity of the frits and from the mixing effect of the frit at the column ends, whereas σ_{bed}^2 comes from the zone broadening of the analyte is it travels through the column bed. These variances are either temporal (σ_t^2) or volumetric (σ_V^2), because the spatial variance (σ_z^2) is not additive.

As the analyte migrates in the column, its band variance increases linearly with the distance traveled. The longitudinal variance is expressed as

$$\sigma_{z,bed}^2 = Hz \quad (4)$$

The longitudinal band variance during the parking period t_{park} can be expressed as follows:

$$\sigma_{z,\text{park}}^2 = 2D_{\text{eff}} t_{\text{park}} \quad (5)$$

where D_{eff} is the effective diffusion coefficient of the analyte in the packed bed immersed in the mobile phase.

When the calculated longitudinal band variance is plotted against the penetration distance, a linear correlation is observed, and the local plate height of the packing bed is determined from the slope of that straight line. The intercept of the line gives the contributions of peak parking and column ends.

$$\sigma_{z,app}^2 = \sigma_{z,end,app}^2 + 2D_{eff} t_{park} + 2Hz \quad (6)$$

Because of the nature of column packing procedure, one may suppose that the inlet and outlet ends of the columns show a different band variance [13].

3. Experimental

The chromatographic analyses were performed on Waters Acquity I Class (Waters Corporation, Milford, MA, USA) instrument. The system consists of a binary solvent manager, an autosampler with a flow-through-needle injector, a column manager, diode-array detector, and a computer data station with Empower 3 software.

In the present study, six reversed phase Waters C_{18} columns – three CORTECS and three XBridge – were tested, which are commercially available. The columns were packed under optimized conditions. The column dimensions were 2.1 × 50, 100, and 150 mm, with 1.6 μm superficially porous particles in case of the CORTECS columns and 1.7 μm fully porous particles (BEH) for XBridge columns.

During the measurements – in the case of the plate height measurements, peak parking and flow-reversal experiments, too – the mobile phase was premixed 90:10 % (v/v) HPLC grade acetonitrile and water (VWR International). The column thermostat was set at 25 °C, while the injection volume was 0.2 μL for each measurement.

The sample was thiourea in each case, which was prepared from analytical standard purchased from Sigma–Aldrich. Thiourea is a non-retained marker for the determination of the column void volume in reversed-phase liquid chromatography. The sample concentration was 0.01 mg/mL and the composition of the sample solvent was identical to the eluent composition.

4. Calculations

The σ_t^2 values were calculated from the second central temporal moments, which were determined by fitting an exponentially modified Gaussian (EMG) peak to the measured data with PeakFit 4.12 software. These fitted values were derived from the average of three parallel measurements in each case, where the RSDs were between ±1.2–1.8%. In addition these values were corrected for the extra-column band broadening $\sigma_{V,\text{system}}^2 = 0.73\ \mu\text{L}^2$, which was measured with a zero volume connection after injecting thiourea.

5. Results and discussion

5.1. Plate height measurements

During the test of the examined columns, the first step was the measurements of the *H–u* curves and the determination of the optimum plate height values, using thiourea as a sample to determine the optimum flow rate of each individual column for the further tests, while the flow rate was changed between 0.05 and 0.6 mL/min (except for the 15-cm-long columns – in that case the maximum flow rate was 0.35 mL/min). The minimum plate height values and the maxima of the plate numbers are reported in Table 1 for each column. The plate height curves are shown in Fig. S1 of Supporting information. Based on the results, 0.25 mL/min flow rate value was chosen for further measurements, because the optima of the columns were found around 0.2–0.3 mL/min flow rate.

5.2. Peak parking experiments

During the peak parking measurements, the sample was injected and eluted ($F_v = 0.25$ mL/min) until the sample zone reached the center of the column. At that time the mobile phase flow was arrested for a time called parking time t_{park}, during which the sample band diffused in the column. When t_{park} (2, 5, 10, 30, 45, or 60 min) has passed, the elution was resumed at the same flow rate until the sample left the column. Details of the peak parking method are described elsewhere [13] and the results of the experiments are presented in Fig. S2 of Supporting information.

Table 1
The characteristics and kinetic performance of the examined columns for the employed eluent composition and flow rate.

	d_p [μm]	Void volume [μL]	Total porosity	Optimum flow rate [mL/min]	N (optimum)	H_{min} [μm]
XBridge 5 cm	1.7	97.6	0.56	0.2	12 300	4.1
XBridge 10 cm	1.7	203.6	0.58	0.3	32 300	3.1
XBridge 15 cm	1.7	289.4	0.55	0.3	48 700	3.1
CORTECS 5 cm	1.6	78.6	0.45	0.2	12 000	4.2
CORTECS 10 cm	1.6	161.1	0.46	0.2	20 200	4.9
CORTECS 15 cm	1.6	237.9	0.46	0.3	57 300	2.6

Table 2
The results of the peak parking and flow-reversal experiments.

	$H_{forward}$ [μm]	$H_{backward}$ [μm]	$\sigma^2_{V,bed,forward}$ [μL²]	$\sigma^2_{V,bed,backward}$ [μL²]	$\sigma^2_{V,end,inlet}$ [μL²]	$\sigma^2_{V,end,outlet}$ [μL²]	$\sigma^2_{V,total,forward}$ [μL²]	$\sigma^2_{V,total,backward}$ [μL²]	$\sigma^2_{V,park}$ [μL²]
XBridge 5 cm	2.592	2.743	0.494	0.523	0.411	0.454	3.282	3.396	1.235
XBridge 10 cm	2.845	2.920	1.179	1.211	0.736	0.679	4.647	4.565	1.266
XBridge 15 cm	3.255	3.018	1.817	1.684	0.386	0.468	4.579	4.612	1.261
CORTECS 5 cm	1.806	1.602	0.223	0.197	0.191	0.182	1.962	1.908	0.615
CORTECS 10 cm	1.546	1.713	0.401	0.445	0.316	0.330	2.528	2.600	0.764
CORTECS 15 cm	2.228	1.839	0.840	0.693	0.527	0.508	3.425	3.122	0.794

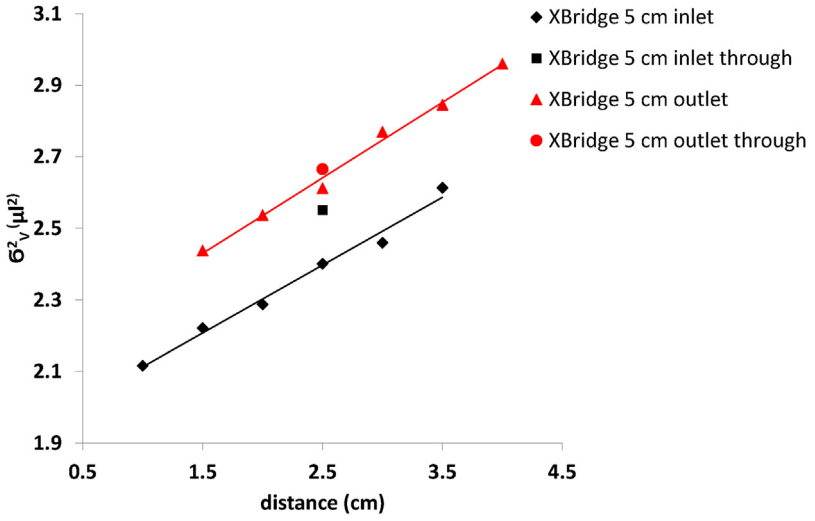

Fig. 1. Volumetric band variance obtained for the 5 cm XBridge column with flow reversal, including 2 min stopped flow. The symbols at the center of the column indicate the variance obtained without flow reversal but also including 2 min stopped flow.

The various columns showed rather similar effective diffusivity values, between $D_{eff} = 1.03–1.35 \times 10^{-5}$ cm²/s. Based on this graph, we calculated the $\sigma^2_{V,park}$ values for the selected parking time (120 s) from the slopes using Eq. (5) and we converted the results to μL² units using Eqs. (1)–(2). In the further calculations, these $\sigma^2_{V,park}$ values for each column were used to determine the other band broadening effects based on Eq. (3). The results are summarized in Table 2.

From these results we can conclude that peak parking has about 50% smaller band broadening effect (expressed in μL²) in the columns packed with core–shell particles compared to the columns packed with fully porous particles. These results were expected because 20% of the column volume is filled by the solid cores (see Table 1) which is not available for the analytes or mobile phase, and the presence of the spherical cores leads to the obstruction of axial diffusion [16]. The remaining 30% differences can be derived from the smaller internal particle porosity of core-shell particles [17].

5.3. Flow-reversal experiments

During these measurements, the column inlets and outlets were tested with an unretained marker, thiourea. The sample was injected and the flow was stopped when the sample zone penetrated a given distance, the column was inverted and after two minutes arrested flow, the non-retained marker was eluted at the same column end where it entered [13]. Besides these flow-reversal measurements, injections were made with standard flow direction at the column inlet and outlet, respectively. From those measurements the σ^2_{total} values were determined, which were used in further calculations according to Eq. (3).

A peak compression effect is observed with the flow-reversal experiments in case of these columns packed with sub-2-μm particles, which originates from the compensation of the multipath dispersion effect and from the radial flow heterogeneity [18,13].

In order to characterize the band broadening occurring at the column ends, a series of measurements were carried out with different penetration distances and with 2 minutes arrested flow, when the flow was reversed. In case of thiourea, 2-minute parking time is enough for the diffusion and the reversal of the flow can be managed during that time too. For such small molecules, the parking time has no further influence on our measurements. When the longitudinal variance is plotted against the penetration distance, the slope of the curves will be directly suitable for the determination of the local plate height. The intercept of the lines

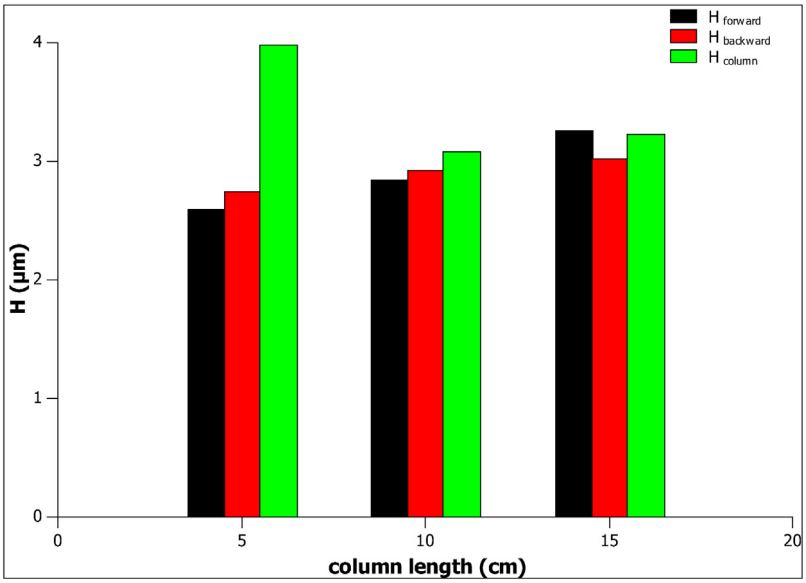

Fig. 2. Comparison of the local plate heights obtained with the flow-reversal method and the overall plate heights of the XBridge columns.

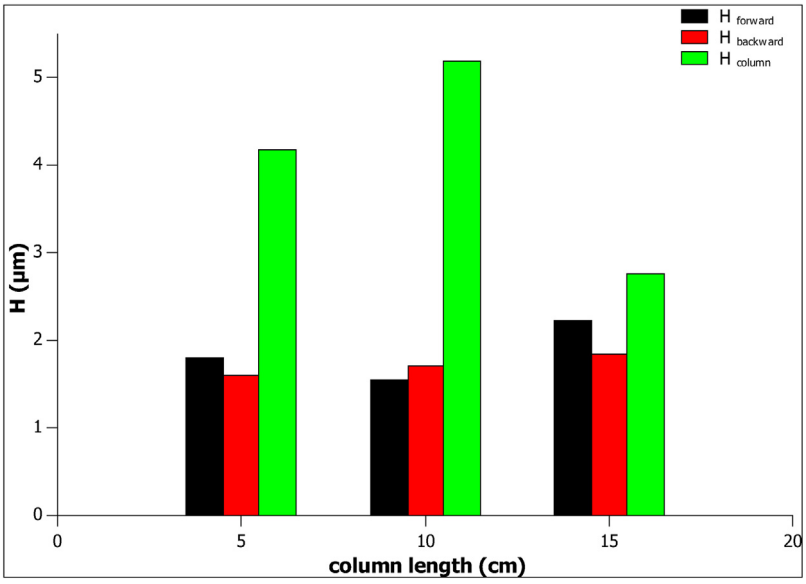

Fig. 3. Comparison of the local plate heights obtained with the flow-reversal method and the overall plate heights of the CORTECS columns.

corrected for the parking effect gives σ^2_{end}. This is, however, not the real zone width in the frits, because the linear velocity is different there since the porosity of the frits differs from that of the packed bed. Therefore Eq. (2) was used to determine σ^2_{end} at both the inlet and outlet, respectively, for which the other contributions had to be calculated first.

The results for the 5-cm-long XBridge column are shown in Fig. 1. The results are expressed in volumetric variance units (μL^2) and the calculated results are presented in Table 2. The further results obtained for the additional five columns are available in Figs. S3–S9 of Supporting information.

The total variances σ^2_{total} that are plotted with different symbols at the center of the column were obtained when the flow was arrested for 2 min but the flow was not reversed, thus no zone compression effect was observed. The plotted lines run roughly parallel, however, we always observed some differences for the local plate height.

The most remarkable differences were detected in the local plate height for the longest columns (15-cm-long XBridge and CORTECS columns). Furthermore, an increasing tendency can be observed for the local plate heights (see in Figs. 2 and 3) with increasing column length, except for the inlet of the 10-cm-long CORTECS column, but that column showed unusual behavior during the *H–u* curve measurements as well. These figures also show differences between the local plate heights ($H_{bed,forward}$ when the column was used in the direction recommended by the manufacturer and $H_{bed,backward}$, when the column was used against the recommended direction) obtained by the flow-reversal method and the overall plate heights obtained for the *H–u* curve (H_{column}), which values contain the effect of the column ends too.

The shorter the column the larger the differences are between these $H_{bed,forward}$ or $H_{bed,backward}$ and H_{column} values except for the 10-cm-long CORTECS column and for the 15-cm-long XBridge column. These differences show the effect of the frits and the column

end structure near the frits for each column, which are larger for the CORTECS columns.

The σ^2_{bed} values were much smaller for the CORTECS columns than for the XBridge columns, due to the nature of the superficially porous particles. Gritti et al. estimated in 2015 that the intrinsic reduced plate height values (free from system and frit contributions) of CORTECS C_{18} 1.6 μm and XBridge C_{18} 1.7 μm in 2.1 internal diameter and 5 cm long column are close to 0.7 and 1.2, respectively, for a non-retained compound. As a matter of fact, packing superficially porous particles such as CORTECS with reduced plate height around or less than 1.0 can be done routinely with short (2–5 cm long) columns [19].

Our present work confirms those results and also demonstrates that the intrinsic reduced plate height of the CORTECS and XBridge particles when packed in 5-cm-long columns is around 1.0 and 1.4 after correcting for frit dispersion (see Table 2).

The σ^2_{end} values obtained for the inlets and outlets are always different, but the differences are rather small, therefore we could not determine which end has a better performance. It was even noticeable that the longer the column the greater the difference between the two ends is. The σ^2_{end} values were much smaller for the CORTECS columns than for the XBridge columns.

These results are shown in Table 2. The results agree well with the findings of Gritti et al. who concluded that radial heterogeneity appears to be controlled by the column length. The longer the column, the larger the relative velocity biases are [14].

6. Conclusion

The kinetic performance of a series of 2.1 × 50, 100, and 150 mm columns packed with fully and superficially porous particles were tested and compared. The CORTECS columns provide a slightly greater plate height values at the optimum mobile phase velocity (except of the CORTECS 15 cm column). The flow reversal method was introduced to characterize the sample zone broadening, the intrinsic plate heights and the differences between the respective column ends. The local plate height values were found smaller with flow reversal than with arrested flow, due to the compensation of the multipath dispersion effect and radial flow profile heterogeneities. We found in every case that efficiency at the respective column ends and the efficiency of the packed bed – i.e. the local plate heights – differ from each other; the columns are heterogeneous, but the difference is negligible, and one can not be sure whether the column inlet or outlet performs better.

The local plate height increases with increasing column length. Comparing these local plate heights to the overall column plate heights we can establish the effect of the frits and the column end structure near the frits, which are larger for the CORTECS columns.

Furthermore, we can conclude shorter columns can be packed with better bed efficiency. The results show that the column length has an influence on heterogeneity and the shorter the column, the more significant the effect of the frits is. Accordingly, although the packed beds in shorter columns are more homogeneous and the local plate heights are smaller for short than for long columns, the overall efficiency of the short columns is worse than that of the long columns since the relative contribution of the frits is more substantial for short columns.

Acknowledgements

The work was supported by the NKFIH OTKA grant K125312. The work was also supported by the ÚNKP-18-3-I-PTE-125 New National Excellence Program of the Ministry of Human Capacities. The authors thank Waters Corporation for the generous gift of the columns used in the experiments.

Appendix A. Supplementary data

Supplementary data associated with this article can be found, in the online version, at https://doi.org/10.1016/j.chroma.2019.05.040.

References

[1] J.W. Thomson, J.S. Mellors, J.W. Eschelbach, J. Joregenson, Recent advances in ultrahigh-pressure liquid chromatography, LCGC N. Am. 24 (2006) 16–20.
[2] J. De Vos, K. Broeckhoven, S. Eeltink, Advances in ultrahigh-pressure liquid chromatography and system design, Anal. Chem. 88 (2016) 262–278.
[3] X. Li, Method Development for High Performance Liquid Chromatography: Novel Organic Modifiers and Column Packing Conditions, Digital Repository @ Iowa State University, 1996 https://lib.dr.iastate.edu/rtd/11159.
[4] G. Crescentini, A.R. Mastrogiacomo, Liquid chromatography capillary columns dry-packed with polar and nonpolar stationary phases, J. Microcolumn Sep. 3 (1991) 539–545.
[5] Y. Guan, L. Zhou, Z. Shang, Dry-packed capillary columns for micro HPLC, J. Sep. Sci. 15 (1992) 434–436.
[6] D. Johnson, Column packing – changing art to science, Genet. Eng. Biotechnol. N. 35 (2015) 24–25.
[7] M.F. Wahab, D.C. Patel, R.M. Wimalysinghe, D.W. Armstrong, Fundamental and practical insights on the packing of modern high-efficiency analytical and capillary columns, Anal. Chem. 89 (2017) 8177–8191.
[8] F. Gritti, M.F. Wahab, Understanding the science behind packing high-efficiency columns and capillaries: facts, fundamentals, challenges, and future directions, LCGC N. Am. 36 (2018) 82–98.
[9] J.J. Kirkland, J.B. Adams, M.A. van Straten, H.A. Claessens, Bidentate silane stationary phases for reversed-phase high-performance liquid chromatography, Anal. Chem. 70 (1998) 4344–4352.
[10] M. Kaminski, Simple test for determination of the degree of distortion of the liquid-phase flow profile in columns for preparative liquid chromatography, J. Chromatogr. A 589 (1992) 61–70.
[11] H. Guo, D.D. Frey, Interpreting the difference between conventional and bi-directional plate-height measurements in liquid chromatography, J. Chromatogr. A 1217 (2010) 6214–6229.
[12] D.K. Roper, E.N. Lightfoot, Estimating plate heights in stacked-membrane chromatography by flow reversal, J. Chromatogr. A 702 (1995) 39–80.
[13] N. Lambert, S. Miyazaki, M. Ohira, N. Tanaka, A. Felinger, Comparison of the kinetic performance of different columns for fast liquid chromatography, emphasizing the contributions of column end structure, J. Chromatogr. A 1473 (2016) 99–108.
[14] F. Gritti, M. Dion, A. Felinger, M. Savaria, Characterization of radial and axial heterogeneities of chromatographic columns by flow reversal, J. Chromatogr. A 1567 (2018) 164–176.
[15] F. Gritti, M. Gilar, Impact of frit dispersion on gradient performance in high-throughput liquid chromatography, J. Chromatogr. A 1591 (2019) 110–119, http://dx.doi.org/10.1016/j.chroma.2019.01.021.
[16] F. Gritti, G. Guiochon, Mass transfer kinetics, band broadening and column efficiency, J. Chromatogr. A 1221 (2012) 2–40.
[17] A. Liekens, J. Denayer, G. Desmet, Experimental investigation of the difference in b-term dominated band broadening between fully porous and porous-shell particles for liquid chromatography using the effective medium theory, J. Chromatogr. A 1218 (2011) 4406–4416.
[18] J.C. Giddings, Dynamics of Chromatography, Part I: Principles and Theory, Marcel Dekker, New York, 1965.
[19] F. Gritti, T. McDonald, M. Gilar, Impact of the column hardware volume on resolution in very high pressure liquid chromatography non-invasive investigations, J. Chromatogr. A 1420 (2015) 54–65.